Novel Organotransition-Metal Cluster Complexes via Reactions of Dinuclear Metal Carbonyls with (μ-σ,π-Alkynyl)(μ-alkanethiolato)bis(tricarbonyliron) Complexes

Dietmar Seyferth* and Jeffrey B. Hoke

Department of Chemistry, Massachusetts Institute of Technology, Cambridge, Massachusetts 02139

Arnold L. Rheingold*

Department of Chemistry, University of Delaware, Newark, Delaware 19716

Martin Cowie* and Allen D. Hunter

Department of Chemistry, University of Alberta, Edmonton, Alberta, Canada T6G 2G2

Received January 22, 1988

The reactions of a series of acetylide-bridged complexes, [(μ_2-C≡CR)(μ_2-^{t}BuS)$Fe_2(CO)_6$] (R = $SiMe_3$ (1), Ph (3), ^{t}Bu (5)) with $Co_2(CO)_8$ and $Fe_2(CO)_9$ have been investigated, and the structures of four products have been determined by X-ray crystallography. Reaction of 1 and $Co_2(CO)_8$ yields the trinuclear species [(μ_3-C≡CSiMe_3)$CoFe_2(CO)_9$] (2). This 48-electron complex has a closed triangular structure in which the acetylide group is σ-bound to Co and π-bound to both Fe atoms. With compound 3 and $Co_2(CO)_8$ the tetranuclear product [(μ_4-C≡CPh)(μ_2-^{t}BuS)$Co_2Fe_2(CO)_{11}$] (4) was obtained. This 64-electron cluster has a spiked triangular structure that can be derived from a tetrahedron by cleavage of both bonds from one iron to the Co atoms. The acetylide group is σ-bound to both irons and π-bound to both cobalts. The reaction of 5 with $Co_2(CO)_8$ yields a mixture of both corresponding tri- and tetranuclear clusters. It appears that the formation of the mixed tri- or tetranuclear clusters depends on the size of the acetylide substituent, with larger substituents destabilizing the tetranuclear cluster with respect to the trinuclear species. Reaction of 3 with $Fe_2(CO)_9$ yields the unusual open triiron cluster, [(μ_3-C≡CPh)(μ_2-^{t}BuS)$Fe_3(CO)_9$] (8). The phenylacetylide group is σ-bound to two irons, which are simultaneously bridged by the thiolato group, and is π-bound to the other iron. If the acetylide group is considered as a three-electron donor, the open, 48-electron structure is unexpected; however, if this group is a five-electron donor, then the open structure is anticipated. In the reaction of 5 with $Fe_2(CO)_9$ the complex [(μ_3-C≡C^{t}Bu)(μ_2-^{t}BuS)$Fe_3(CO)_9$] (9) is obtained. The acetylide group is σ-bound to one iron and π-bound to the two others so it clearly functions as a five-electron donor resulting in an open triangular structure. Crystallographic data for the four species are as follows. 2: triclinic, $P\bar{1}$, a = 9.046 (2) Å, b = 9.509 (2) Å, c = 11.721 (3) Å, α = 101.41 (2)°, β = 97.58 (2)°, γ = 90.64 (2)°, Z = 2, NO = 2772, R = 0.036, R_w = 0.042. 4: monoclinic $P2_1/c$, a = 14.303 (4) Å, b = 11.710 (3) Å, c = 16.462 (4) Å, β = 97.86 (2)°, Z = 4, NO = 3299, R = 0.046, R_w = 0.049. 8: orthorhombic $Pbca$, a = 14.413 (2) Å, b = 23.269 (2) Å, c = 14.551 (1) Å, Z = 8, NO = 3224, R = 0.024, R_w = 0.030. 9: monoclinic $P2_1/c$, a = 10.000 (1) Å, b = 14.953 (2) Å, c = 16.299 (1) Å, β = 102.364 (7)°, Z = 4, NO = 3816, R = 0.027, R_w = 0.035.

Introduction

In a previous paper[1] we described the preparation of some acetylide-bridged complexes of the type (μ-σ,π-alkynyl)(μ-alkanethiolato)bis(tricarbonyliron) and their subsequent reactions with some Lewis bases. Previous work, in which the reactions of diverse transition-metal acetylide complexes with metal carbonyls were used to good advantage for the preparation of higher nuclearity, homo and heterometallic acetylide cluster complexes,[2] encouraged us to consider such an approach utilizing the above acetylide-bridged species. The results of this study, which indicate that the products obtained from the reactions with dicobalt octacarbonyl and diiron nonacarbonyl depend not only on the metal carbonyl used but also on the alkynyl group of (μ-R′C≡C)(μ-RS)$Fe_2(CO)_6$, are presented herein.

Results and Discussion

Reaction of (μ-σ,π-C≡CSiMe_3)(μ-^{t}BuS)$Fe_2(CO)_6$ (1) with dicobalt octacarbonyl at room temperature in THF generated the heterometallic, trinuclear acetylide complex (μ_3,η^2-C≡CSiMe_3)$CoFe_2(CO)_9$ (2) in 87% yield (eq 1). This product is rather unusual in several ways. Not only has only one of the cobalt atoms become incorporated into

Table I. Relevant Bond Distances (Å) for 2

Fe(1)–Fe(2)	2.494 (1)	Fe(2)–C(14)	2.012 (4)
Fe(1)–Co	2.628 (1)	Fe(1)–C(14)	2.012 (4)
Fe(2)–Co	2.630 (1)	Co–C(14)	1.821 (4)
Fe(2)–C(13)	2.133 (4)	C(13)–C(14)	1.289 (6)
Fe(1)–C(13)	2.129 (4)	C(13)–Si	1.862 (4)
Fe(1)–CO(mean)	1.796 (5)	Fe(2)C–O(mean)	1.135 (5)
Fe(1)C–O(mean)	1.132 (7)	Co–CO(mean)	1.803 (6)
Fe(2)–CO(mean)	1.796 (6)	CoC–O(mean)	1.121 (7)

Table II. Relevant Bond Angles (deg) for 2

Fe(2)–Fe(1)–Co	61.7 (1)	Fe(2)–C(13)–Si	136.6 (2)
Co–Fe(2)–Fe(1)	61.6 (1)	C(14)–Fe(2)–Co	43.7 (1)
Fe(2)–Co–Fe(1)	56.6 (1)	C(14)–Fe(1)–Co	43.8 (1)
Co–C(14)–Fe(1)	86.4 (2)	C(14)–Fe(2)–C(13)	36.1 (2)
Co–C(14)–Fe(2)	86.5 (2)	C(14)–Fe(1)–C(13)	36.1 (2)
Co–C(14)–C(13)	158.8 (3)	C(14)–Fe(1)–Fe(2)	51.7 (1)
Fe(1)–C(14)–C(13)	76.9 (1)	C(14)–Fe(2)–Fe(1)	51.7 (1)
Fe(2)–C(14)–C(13)	77.1 (3)	C(13)–Fe(1)–Co	79.3 (1)
Fe(1)–C(14)–Fe(2)	76.6 (1)	C(13)–Fe(2)–Co	79.1 (1)
Fe(1)–C(13)–C(14)	67.0 (2)	C(13)–Fe(2)–Fe(1)	54.1 (1)
Fe(2)–C(13)–C(14)	66.8 (2)	C(13)–Fe(1)–Fe(2)	54.3 (1)
Fe(1)–C(13)–Fe(2)	71.6 (1)	C(14)–Co–Fe(2)	49.8 (1)
C(14)–C(13)–Si	145.6 (3)	C(14)–Co–Fe(1)	49.8 (1)
Fe(1)–C(13)–Si	136.2 (2)		

(1) Seyferth, D.; Hoke, J. B. *J. Organomet. Chem.*, in press.

(2) (a) Yasufuku, K.; Yamazaki, H. *Bull. Chem. Soc. Jpn.* **1972**, *45*, 2664. (b) Yasufuku, K.; Yamazaki, H. *Bull. Chem. Soc. Jpn.* **1975**, *48*, 1616. (c) ten Hoedt, R. W. M.; Noltes, J. G.; van Koten, G.; Spek, A. L. *J. Chem. Soc., Dalton Trans.* **1978**, 1800. (d) Abu Salah, O. M.; Bruce, M. I.; Churchill, M. R.; Bezman, S. A. *J. Chem. Soc., Chem. Commun.* **1972**, 858. (e) Abu Salah, O. M.; Bruce, M. I.; Churchill, M. R.; De Boer, B. G. *J. Chem. Soc., Chem. Commun.* **1974**, 688. (f) Marinetti, A.; Sappa, E.; Tiripicchio, A.; Camellini, M. T. *J. Organomet. Chem.* **1980**, *197*, 335.

0276-7333/88/2307-2163$01.50/0

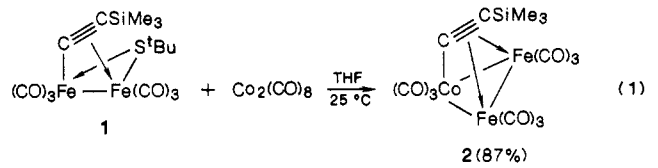

the product, but even more unexpectedly, the thiolate ligand of **1** has been lost completely. Furthermore, whereas the acetylide ligand was σ-bound to iron in **1**, it is now σ-bound to cobalt in **2**. Subsequent bonding to the two iron atoms of the cluster then occurs through donation from the acetylide triple bond. The structure of **2** has been confirmed by X-ray crystallography and is shown in Figure 1; pertinent bond distances and angles are given in Tables I and II, respectively. The most striking feature of this molecule from a crystallographic viewpoint is the virtual plane of symmetry bisecting the Fe(1)–Co–Fe(2) angle and containing the Co, C(14), C(13), and Si atoms. As expected, the C(13)–C(14) bond distance of 1.289 (6) Å is longer than that of an uncoordinated acetylene,[3] while the corresponding Co–C(14) bond distance of 1.821 (4) Å is very short or "carbene-like". Similar trends have been observed in related triiron acetylide complexes as well.[2a,b,4,5] The "carbene-like" nature of the Co–C(14) bond is aptly illustrated by the downfield shift of the C(14) resonance (δ_C 202.60) in the ^{13}C NMR spectrum. Conversely, the C_β resonance occurs far upfield (δ_C 97.43) consistent with other μ_3,η^2-acetylide complexes of this general type.[4-6] Finally, in the infrared spectrum, a strong band is observed at 1663 cm^{-1} which can be assigned to the carbon–carbon stretch of the coordinated triple bond, consistent with a decrease in frequency from that of a free acetylene.

Surprisingly, reaction of the closely related complex (μ-σ,π-C≡CPh)(μ-^{t}BuS)$Fe_2(CO)_6$ (**3**) with dicobalt octacarbonyl did not produce the corresponding triply bridging phenylacetylide derivative of type **2** but instead generated the unusual heterometallic, tetranuclear "acetylide" complex (μ_4-C≡CPh)(μ-CO)(μ-^{t}BuS)$Co_2Fe_2(CO)_{10}$ (**4**) in 65% yield (eq 2), as confirmed by the X-ray structure determination. An ORTEP plot showing the atom-labeling scheme appears in Figure 2 while pertinent bond distances and angles are given in Tables III and IV, respectively.

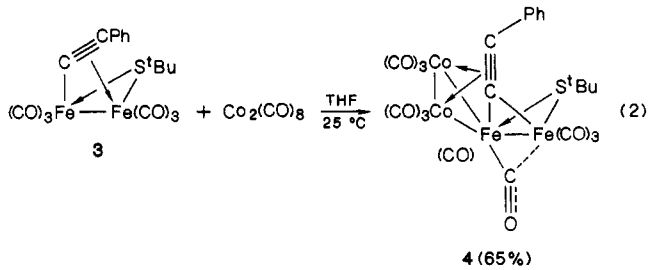

This species is much closer to what might be expected upon reaction of the diiron species **1** with $Co_2(CO)_8$; in particular both cobalt atoms remain in the product and the thiolate group still bridges the iron atoms. Nevertheless several unexpected transformations have taken place. Most noteworthy among these perhaps is that the α-carbon of the acetylide group is now σ-bound to *both* Fe

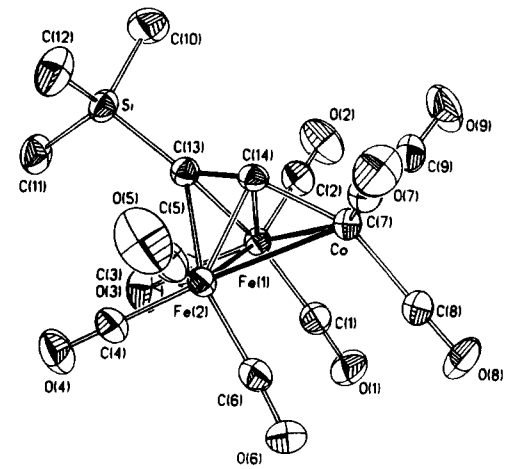

Figure 1. Perspective view of compound **2** showing the numbering scheme. Thermal ellipsoids are drawn at the 40% level; hydrogens are omitted.

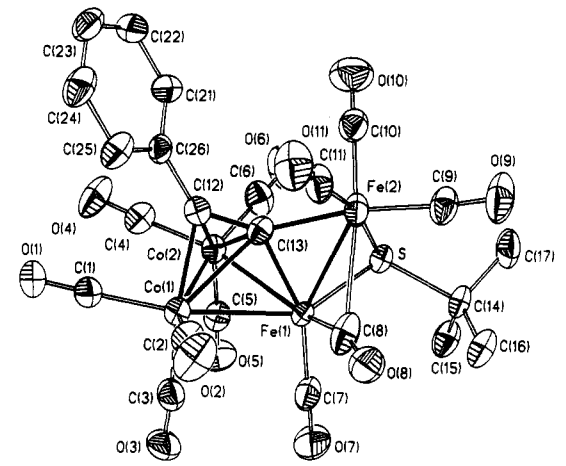

Figure 2. View and numbering scheme for compound **4**. Thermal ellipsoids shown at the 40% level; hydrogen atoms are omitted.

Table III. Relevant Bond Distances (Å) for 4

Co(1)–Co(2)	2.478 (1)	C(8)–O(8)	1.118 (8)
Co(1)–Fe(1)	2.596 (1)	Fe(2)–C(13)	2.022 (5)
Co(2)–Fe(1)	2.643 (1)	Fe(1)–C(13)	1.912 (5)
Fe(1)–Fe(2)	2.508 (1)	C(12)–C(13)	1.322 (8)
Fe(1)–S	2.217 (1)	Co(1)–C(13)	2.305 (5)
Fe(2)–S	2.281 (2)	Co(2)–C(13)	2.031 (5)
S–C(14)	1.882 (6)	Co(1)–C(12)	2.015 (5)
Fe(1)–C(8)	1.830 (6)	Co(2)–C(12)	2.052 (5)
Fe(2)–C(8)	2.458 (7)	C(12)–C(26)	1.472 (7)
Fe(1)–C(7)	1.789 (7)	Fe(2)–CO(mean)	1.802 (8)
C(7)–O(7)	1.129 (9)	Fe(2)C–O(mean)	1.129 (6)
Co(2)–CO(mean)	1.797 (6)	Co(1)–CO(mean)	1.802 (6)
Co(2)C–O(mean)	1.128 (8)	Co(1)C–O(mean)	1.129 (8)

atoms while also being π-bound to both Co atoms such that the acetylide group lies almost perpendicular to the Co–Co bond. As a result all four metal atoms are within bonding distance of C(13). Furthermore, one carbonyl group on Fe(1) has been substituted by the "$Co_2(CO)_6$" fragment and one of those remaining has moved into a semibridging position with Fe(2). This semibridging carbonyl is much closer to Fe(1) than to Fe(2) (1.830 (6) vs 2.458 (7) Å), apparently in order to relieve some of the electron deficiency of Fe(1). Both other groups that are bridging the Fe(1)–Fe(2) bond are also unsymmetrically bonded and are again closer to Fe(1), with Fe–S distances of 2.217 (1) and 2.281 (2) Å, and distances to the α-carbon of the acetylide group of 1.912 (5) and 2.002 (5) Å. As expected, the C(12)–C(13) bond of 1.322 (8) Å is considerably longer

(3) *International Tables for X-ray Crystallography*; MacGillavry, C. M., Rieck, G. D., Eds.; Kynoch: Birmingham, England, 1974; Vol. 3, p 276.
(4) (a) De Montauzon, D.; Mathieu, R. *J. Organomet. Chem.* **1983**, *252*, C83. (b) Alami, M. K.; Dahan, F.; Mathieu, R. *Organometallics* **1985**, *4*, 2122.
(5) Hriljac, J.; Shriver, D. F. *Organometallics* **1985**, *4*, 2225.
(6) Carty, A. J. *Pure Appl. Chem.* **1982**, *54*, 113.

Table IV. Relevant Bond Angles (deg) for 4

Fe(2)-Fe(1)-Co(1)	105.1 (1)	C(13)-Co(1)-Co(2)	50.1 (1)
Fe(2)-Fe(1)-Co(2)	94.9 (1)	C(13)-Co(2)-Co(1)	60.5 (1)
Fe(1)-Co(2)-Co(1)	60.8 (1)	Co(1)-C(13)-C(12)	60.5 (3)
Fe(1)-Co(1)-Co(2)	62.7 (1)	Co(2)-C(13)-C(12)	72.0 (3)
Co(2)-Fe(1)-Co(1)	56.4 (1)	Fe(2)-C(13)-Co(1)	139.0 (2)
S-Fe(1)-Fe(2)	57.3 (1)	Fe(2)-C(13)-Co(2)	138.9 (3)
Fe(1)-Fe(2)-S	54.9 (1)	Fe(2)-C(13)-C(12)	142.2 (4)
Fe(1)-S-Fe(2)	67.8 (1)	C(13)-Co(1)-Fe(1)	45.4 (1)
Fe(1)-C(8)-Fe(2)	69.8 (2)	C(13)-Co(2)-Fe(1)	46.0 (2)
Fe(1)-Fe(2)-C(8)	43.2 (2)	C(13)-Fe(1)-S	89.5 (2)
Fe(2)-Fe(1)-C(8)	66.9 (2)	C(13)-Fe(2)-S	85.0 (2)
Fe(2)-Fe(1)-C(13)	52.4 (1)	C(13)-Fe(1)-C(8)	99.4 (3)
Fe(1)-Fe(2)-C(13)	48.5 (2)	C(13)-Fe(2)-C(8)	78.5 (2)
Fe(2)-C(13)-Fe(1)	79.2 (2)	C(13)-C(12)-Co(1)	84.7 (3)
Fe(1)-C(13)-Co(1)	75.4 (2)	C(13)-C(12)-C(26)	137.0 (5)
Fe(1)-C(13)-Co(2)	84.1 (2)	Co(1)-C(12)-C(26)	131.4 (3)
Fe(1)-C(13)-C(12)	134.7 (4)	Co(2)-C(12)-C(26)	133.2 (3)
Co(1)-C(13)-Co(2)	69.4 (2)	S-Fe(1)-Co(1)	145.5 (1)
C(13)-Fe(1)-Co(1)	59.2 (2)	S-Fe(1)-Co(2)	93.2 (1)
C(13)-Fe(1)-Co(2)	49.9 (2)	Fe(1)-Co(1)-C(12)	79.9 (2)
C(13)-Co(1)-C(12)	34.8 (2)	Fe(1)-Co(2)-C(12)	78.1 (2)
C(13)-Co(2)-C(12)	37.8 (2)		

than in an uncoordinated acetylene and very much resembles a normal C=C double bond.[3] The Co(1)-Co(2) distance of 2.478 (1) Å is quite short although it is consistent with other perpendicular acetylene-dicobalt complexes.[7] Also, the Co(1)-C(12) and Co(2)-C(12) distances are consistent with these simpler dicobalt counterparts, although as can be seen, C(12) is somewhat closer to Co(1) than to Co(2). Conversely, C(13), surprisingly, is much closer to Co(2) than to Co(1) (2.031 (5) vs 2.305 (5) Å). Balancing this effect, Fe(1) bonds somewhat nearer to Co(1) than to Co(2) (2.596 (1) vs 2.643 (1) Å). Although the slightly twisted orientation of the acetylide ligand with respect to the dicobalt axis may be electronic in origin, it seems more likely that it results from nonbonded contacts between the phenyl group of the acetylide ligand and the carbonyl groups (C(10)O(10) and C(11)O(11)) on Fe(2). It may be that such interactions in the case of the bulkier trimethylsilyl derivative are enough to destabilize the analogous species, leading instead to compound **2**.

The spiked triangular structure observed for **4** is consistent with its cluster valence electron count of 64,[8] if the μ_4-acetylide group is considered a five-electron donor, and can be thought of as derived from the closed 60-electron tetrahedron by the cleavage of two M-M bonds (between Fe(2) and both Co atoms in this case). This structure is very analogous to that observed for $[Cp_2Ni_2Fe_2(CO)_5(\mu_2\text{-}PPh_2)(\mu_4\text{-}C{\equiv}CPh)]$[9] except that in this dinickel complex the original Ni_2 framework has not remained intact. However, in both species the two metal atoms defining the "spike" in the cluster are bridged by the thiolato or phosphido groups and are also σ-bonded to the α-carbon of the acetylide group.

As revealed in the ^1H and ^{13}C NMR spectra, **4** is isolated as a mixture of two inseparable isomers which, by analogy to other thiolate-bridged diiron systems, may result from either an axial or an equatorial orientation of the organic thiolate group. Furthermore, in the ^{13}C NMR spectrum, the four acetylide carbon resonances (two for each isomer) are observed in the range of 139-153 ppm, while in the infrared spectrum, the coordinated triple bond gives rise to a band at 1620 cm^{-1}. The semibridging carbonyl ligand likewise gives rise to a strong absorption at 1850 cm^{-1}.[10]

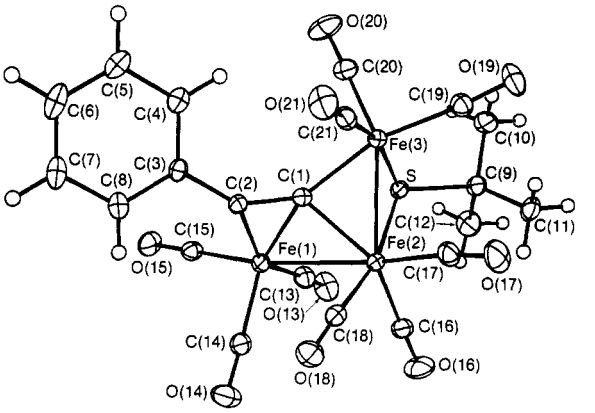

Figure 3. View and numbering scheme for compound **8**. The 20% thermal ellipsoids are shown for all atoms except hydrogens which are drawn artificially small.

In the corresponding reaction of $(\mu\text{-}\sigma,\pi\text{-}C{\equiv}C^tBu)(\mu\text{-}^tBuS)Fe_2(CO)_6$ (**5**) with dicobalt octacarbonyl, products of both types **2** and **4** were isolated in 44% and 30% yields, respectively (eq 3). The spectroscopic and analytical data for these new acetylide complexes, **6** and **7**, were consistent with the structures shown.

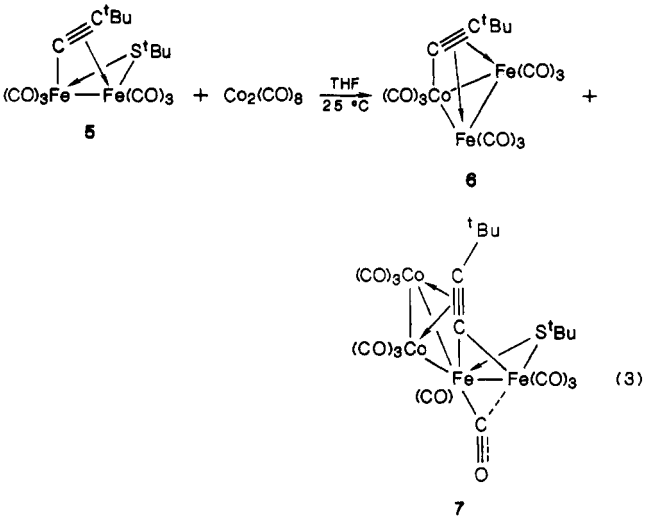

The observations of both products **6** and **7**, in the *tert*-butylacetylide complex is consistent with our previous suggestion of steric destabilization of the tetranuclear species. The *tert*-butyl group is smaller than the trimethylsilyl group, owing to the covalent radii differences between Si (1.17 Å) and C (0.77 Å) yet is bulkier than a phenyl group.[9] It thus seems reasonable to propose that the reaction of the diiron acetylides with dicobalt octacarbonyl proceeds initially to a tetranuclear cluster (of type **4** or **7**). With the smaller phenyl substituent this tetranuclear species (**4**) is stable whereas with the large trimethylsilyl substituent destabilization of the tetranuclear cluster to give the trinuclear cluster **2** occurs. In the case of the intermediate-sized *tert*-butyl substituent both the trinuclear (**6**) and tetranuclear (**7**) products are observed.

The reactions of the diiron acetylide bridged species with $Fe_2(CO)_9$ proceeded much differently than the analogous reactions with $Co_2(CO)_8$ in two important ways. First, only trinuclear products were observed, and second, the bridging thiolato group remained in all products.

(7) Cotton, F. A.; Jamerson, J. D.; Stults, B. R. *J. Am. Chem. Soc.* **1976**, *98*, 1774.
(8) Owen, S. M. *Polyhedron* **1988**, *7*, 253.
(9) Weatherhill, C.; Taylor, N. J.; Carty, A. J.; Sappa, E.; Tiripicchio, A. *J. Organomet. Chem.* **1985**, *291*, C9.
(10) *Principles and Applications of Organotransition Metal Chemistry*; Collman, J. P., Hegedus, L. S., Eds.; University Science Books: Mill Valley, CA, 1980; p 85.

Table V. Bond Lengths (Å) for Compound 8[a]

Fe(1)–Fe(2)	2.6985 (5)	O(14)–C(14)	1.132 (3)
Fe(1)–C(1)	2.059 (3)	O(15)–C(15)	1.138 (3)
Fe(1)–C(2)	1.867 (3)	O(16)–C(16)	1.135 (3)
Fe(1)–C(13)	1.833 (3)	O(17)–C(17)	1.135 (4)
Fe(1)–C(14)	1.787 (3)	O(18)–C(18)	1.141 (3)
Fe(1)–C(15)	1.772 (3)	O(19)–C(19)	1.131 (3)
Fe(2)–Fe(3)	2.5382 (5)	O(20)–C(20)	1.128 (4)
Fe(2)–S	2.2885 (7)	O(21)–C(21)	1.132 (3)
Fe(2)–C(1)	2.019 (3)	C(1)–C(2)	1.324 (3)
Fe(2)–C(16)	1.797 (3)	C(2)–C(3)	1.467 (3)
Fe(2)–C(17)	1.793 (3)	C(3)–C(4)	1.397 (4)
Fe(2)–C(18)	1.790 (3)	C(3)–C(8)	1.380 (4)
Fe(3)–S	2.2463 (8)	C(4)–C(5)	1.378 (4)
Fe(3)–C(1)	1.954 (3)	C(5)–C(6)	1.364 (5)
Fe(3)–C(19)	1.835 (3)	C(6)–C(7)	1.379 (6)
Fe(3)–C(20)	1.783 (3)	C(7)–C(8)	1.390 (4)
Fe(3)–C(21)	1.792 (3)	C(9)–C(10)	1.525 (4)
S–C(9)	1.866 (3)	C(9)–C(11)	1.520 (4)
O(13)–C(13)	1.137 (4)	C(9)–C(12)	1.537 (4)

[a] Numbers in parentheses are estimated standard deviations in the least significant digits.

Reaction of $(\mu\text{-}\sigma,\pi\text{-}C{\equiv}CPh)(\mu\text{-}^tBuS)Fe_2(CO)_6$ (**3**), with diiron nonacarbonyl generated the unusual triiron cluster $(\mu_3,\eta^2\text{-}C{\equiv}CPh)(\mu\text{-}^tBuS)Fe_3(CO)_9$ (**8**) in 91% yield (eq 4).

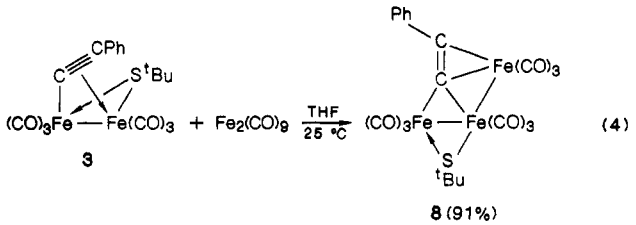

An ORTEP plot summarizing the atom-labeling scheme appears in Figure 3, and structural parameters are given in Tables V and VI. Although the formation of **8** can be envisioned as resulting from the formal insertion of an $Fe(CO)_3$ unit into the electron-rich, iron–acetylide bond of **3**, it seems more likely that some tetranuclear species is the first product, as was observed with $Co_2(CO)_8$, which then loses an iron carbonyl fragment yielding the trinuclear product. In this product the thiolato group still bridges two iron atoms, but the acetylide π bond has moved away from Fe(2) to be replaced by a σ bond with C(1) and a bond to Fe(1). Although in this discussion we have inferred that Fe(2) and Fe(3) derive from **3**, in fact any two of the iron atoms could derive from **3** since we cannot rule out that significant rearrangement of the acetylide and thiolato groups has occurred. In fact rearrangement of the acetylide group in compound **2** has already been noted and rearrangement of a bridging phosphido group, analogous to our thiolato groups, has also been reported.[9] The Fe(1)–Fe(2)–Fe(3) fragment forms an approximate right angle at Fe(2) (94.85 (2)°) such that although Fe(2) is clearly bonded to Fe(1) and Fe(3) (2.6985 (5) and 2.5382 (5) Å), Fe(1) and Fe(3) are clearly outside of normal bonding distance (3.8577 (5) Å). Whereas the α-carbon atom of the resulting "acetylide" ligand is bound to four other atoms, the β-carbon atom is bound to only three, being outside of normal bonding distance to Fe(2) and Fe(3) (3.066 (3) and 3.136 (3) Å, respectively). Once again, a large degree of electron delocalization over the entire cluster framework is indicated, which agrees with the X-ray structure, and no simple Lewis structure adequately accounts for the bonding. As shown by the ^1H and ^{13}C NMR spectra, **8** is isolated as a mixture of two inseparable isomers presumably resulting from an axial or equatorial orientation of the organic thiolate ligand. The carbon atoms of the "acetylide" ligand are observed in the ^{13}C NMR spectrum at 201.24 and 228.61 ppm.

On the basis of the structure determination, which shows that the acetylide group is π-bound to only Fe(1), it appears that the bridging acetylide group in **8** functions as only a three-electron donor. However, this would yield a 48-electron cluster which would be expected to have a *closed* triangular structure[8] as was observed for **2**. The open triangular cluster observed for **8** is therefore rather unusual, unless we consider the acetylide group to be functioning as a five-electron donor, yielding a 50-electron cluster which would be consistent with the open structure.

Table VI. Bond Angles (deg) for Compound 8[a]

Fe(2)–Fe(1)–C(1)	47.93 (7)	S–Fe(2)–C(18)	166.33 (9)	Fe(2)–C(1)–C(2)	132.0 (2)
Fe(2)–Fe(1)–C(2)	82.22 (8)	C(1)–Fe(2)–C(16)	141.8 (1)	Fe(3)–C(1)–C(2)	145.6 (2)
Fe(2)–Fe(1)–C(13)	85.4 (1)	C(1)–Fe(2)–C(17)	119.4 (1)	Fe(1)–C(2)–C(1)	78.3 (2)
Fe(2)–Fe(1)–C(14)	96.90 (9)	C(1)–Fe(2)–C(18)	90.2 (1)	Fe(1)–C(2)–C(3)	139.8 (2)
Fe(2)–Fe(1)–C(15)	171.07 (9)	C(16)–Fe(2)–C(17)	98.6 (1)	C(1)–C(2)–C(3)	140.3 (2)
C(1)–Fe(1)–C(2)	39.1 (1)	C(16)–Fe(2)–C(18)	94.3 (1)	C(2)–C(3)–C(4)	121.3 (2)
C(1)–Fe(1)–C(13)	114.2 (1)	C(17)–Fe(2)–C(18)	88.5 (1)	C(2)–C(3)–C(8)	119.9 (3)
C(1)–Fe(1)–C(14)	127.1 (1)	Fe(2)–Fe(3)–S	56.76 (2)	C(4)–C(3)–C(8)	118.8 (3)
C(1)–Fe(1)–C(15)	124.0 (1)	Fe(2)–Fe(3)–C(1)	51.44 (7)	C(3)–C(4)–C(5)	120.3 (3)
C(2)–Fe(1)–C(13)	147.6 (1)	Fe(2)–Fe(3)–C(19)	112.38 (9)	C(4)–C(5)–C(6)	120.5 (3)
C(2)–Fe(1)–C(14)	114.7 (1)	Fe(2)–Fe(3)–C(20)	140.7 (1)	C(5)–C(6)–C(7)	120.0 (3)
C(2)–Fe(1)–C(15)	91.8 (1)	Fe(2)–Fe(3)–C(21)	105.79 (9)	C(6)–C(7)–C(8)	120.0 (3)
C(13)–Fe(1)–C(14)	96.5 (1)	S–Fe(3)–C(1)	78.59 (8)	C(3)–C(8)–C(7)	120.4 (3)
C(13)–Fe(1)–C(15)	96.4 (1)	S–Fe(3)–C(19)	99.91 (9)	S–C(9)–C(10)	106.2 (2)
C(14)–Fe(1)–C(15)	91.6 (1)	S–Fe(3)–C(20)	96.1 (1)	S–C(9)–C(11)	114.4 (2)
Fe(1)–Fe(2)–Fe(3)	94.85 (2)	S–Fe(3)–C(21)	162.03 (9)	S–C(9)–C(12)	103.5 (2)
Fe(1)–Fe(2)–S	86.89 (2)	C(1)–Fe(3)–C(19)	161.7 (1)	C(10)–C(9)–C(11)	111.6 (3)
Fe(1)–Fe(2)–C(1)	49.20 (7)	C(1)–Fe(3)–C(20)	99.4 (1)	C(10)–C(9)–C(12)	110.1 (3)
Fe(1)–Fe(2)–C(16)	93.8 (1)	C(1)–Fe(3)–C(21)	86.9 (1)	C(11)–C(9)–C(12)	110.6 (3)
Fe(1)–Fe(2)–C(17)	165.3 (1)	C(19)–Fe(3)–C(20)	99.1 (1)	Fe(1)–C(13)–O(13)	175.9 (3)
Fe(1)–Fe(2)–C(18)	82.69 (9)	C(19)–Fe(3)–C(21)	90.7 (1)	Fe(1)–C(14)–O(14)	176.4 (3)
Fe(3)–Fe(2)–S	55.18 (2)	C(20)–Fe(3)–C(21)	96.6 (1)	Fe(1)–C(15)–O(15)	178.9 (3)
Fe(3)–Fe(2)–C(1)	49.16 (7)	Fe(2)–S–Fe(3)	68.07 (2)	Fe(2)–C(16)–O(16)	178.8 (3)
Fe(3)–Fe(2)–C(16)	148.48 (9)	Fe(2)–S–C(9)	120.3 (1)	Fe(2)–C(17)–O(17)	171.8 (3)
Fe(3)–Fe(2)–C(17)	78.6 (1)	Fe(3)–S–C(9)	120.0 (1)	Fe(2)–C(18)–O(18)	178.0 (3)
Fe(3)–Fe(2)–C(18)	116.85 (9)	Fe(1)–C(1)–Fe(2)	82.87 (9)	Fe(3)–C(19)–O(19)	174.4 (3)
S–Fe(2)–C(1)	76.30 (7)	Fe(1)–C(1)–Fe(3)	148.1 (1)	Fe(3)–C(20)–O(20)	178.9 (3)
S–Fe(2)–C(16)	95.2 (1)	Fe(1)–C(1)–C(2)	62.6 (1)	Fe(3)–C(21)–O(21)	179.3 (3)
S–Fe(2)–C(17)	99.8 (1)	Fe(2)–C(1)–Fe(3)	79.41 (9)		

[a] Numbers in parentheses are estimated standard deviations in the least significant digit.

Table VII. Bond Lengths (Å) for Compound 9[a]

Fe(1)–Fe(2)	2.6927 (4)	S–C(7)	1.871 (2)
Fe(1)–S	2.3143 (6)	O(11)–C(11)	1.137 (3)
Fe(1)–C(1)	2.091 (2)	O(12)–C(12)	1.134 (3)
Fe(1)–C(2)	2.277 (2)	O(13)–C(13)	1.131 (3)
Fe(1)–C(11)	1.795 (3)	O(14)–C(14)	1.135 (3)
Fe(1)–C(12)	1.803 (3)	O(15)–C(15)	1.145 (3)
Fe(1)–C(13)	1.801 (3)	O(16)–C(16)	1.135 (3)
Fe(2)–Fe(3)	2.6799 (5)	O(17)–C(17)	1.133 (3)
Fe(2)–C(1)	1.828 (2)	O(18)–C(18)	1.132 (3)
Fe(2)–C(14)	1.792 (3)	O(19)–C(19)	1.141 (3)
Fe(2)–C(15)	1.779 (3)	C(1)–C(2)	1.275 (3)
Fe(2)–C(16)	1.807 (3)	C(2)–C(3)	1.518 (3)
Fe(3)–S	2.3145 (6)	C(3)–C(4)	1.524 (4)
Fe(3)–C(1)	2.096 (2)	C(3)–C(5)	1.526 (4)
Fe(3)–C(2)	2.288 (2)	C(3)–C(6)	1.530 (4)
Fe(3)–C(17)	1.797 (3)	C(7)–C(8)	1.526 (3)
Fe(3)–C(18)	1.790 (3)	C(7)–C(9)	1.530 (4)
Fe(3)–C(19)	1.796 (3)	C(7)–C(10)	1.527 (4)

[a] Numbers in parentheses are estimated standard deviations in the least significant digits.

Reaction of $(\mu\text{-}\sigma,\pi\text{-}C{\equiv}C^tBu)(\mu\text{-}^tBuS)Fe_2(CO)_6$ (**5**) with diiron nonacarbonyl proceeded in an apparently different manner, with the isolation of the new acetylide complex $(\mu_3,\eta^2\text{-}C{\equiv}C^tBu)(\mu\text{-}^tBuS)Fe_3(CO)_9$ (**9**) (eq 5). Once again,

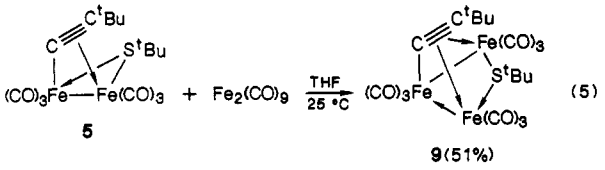

5 **9** (51%)

the structure has been confirmed by X-ray crystallography and is shown in Figure 4. Bond lengths and angles are given in Tables VII and VIII, respectively. The structure of the phenylacetylide derivative **8** is rather different from that of the *tert*-butylacetylide species **9**. Whereas in the rather unsymmetrical species **8** the two carbons of the acetylide moiety bridge one Fe–Fe bond and the thiolato bridges the other, compound **9** is symmetric with both the

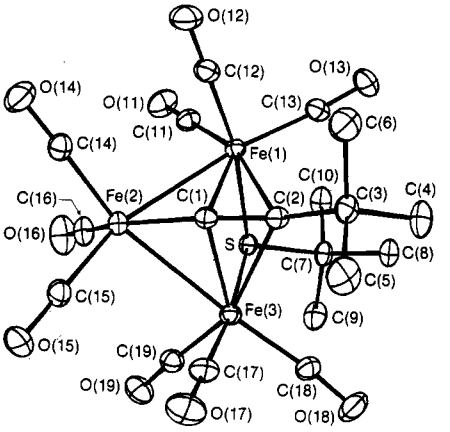

Figure 4. View and numbering scheme for compound **9** The 20% thermal ellipsoids are shown; hydrogens are omitted.

acetylide and the thiolato group bridging the same metals (Fe(1) and Fe(3)). In this case the acetylide is σ-bound to only the central atom of the cluster (Fe(2)) while it is π-bound to Fe(1) and Fe(3). With a separation of 3.1653 (4) Å, Fe(1) and Fe(3) are not connected by a formal Fe-Fe bond, whereas the other two Fe–Fe distances (2.6927 (4) and 2.6799 (5) Å) correspond to normal single bonds. The separation between Fe(1) and Fe(3) is significantly less than that in **8**, and the resulting Fe(1)–Fe(2)–Fe(3) angle, at 72.19 (1)°, is more acute, owing to the two bridging groups in **9** drawing the metals together. A further consequence of the different orientations of the bridging groups is a slight enlargement of the parameters of these bridging groups in **9** where they span two metals which are not mutually bonded. Therefore the Fe–S–Fe angle (86.29 (2)°) and the Fe–S distances (2.3143 (6), 2.3145 (6) Å) in **9** are larger than those in **8** (68.07 (2)° and 2.2885 (7), 2.2463 (8) Å, respectively). Similarly, excluding the one Fe(2)–C(1) σ bond in **9** (1.828 (2) Å), the Fe–acetylide distances in **9** (2.091 (2)–2.288 (2) Å) are larger than those

Table VIII. Bond Angles (deg) for Compound 9[a]

Fe(2)–Fe(1)–S	80.18 (2)	C(1)–Fe(2)–C(15)	108.5 (1)	Fe(1)–C(1)–C(2)	81.2 (1)
Fe(2)–Fe(1)–C(1)	42.63 (6)	C(1)–Fe(2)–C(16)	143.4 (1)	Fe(2)–C(1)–Fe(3)	85.88 (8)
Fe(2)–Fe(1)–C(2)	75.54 (6)	C(14)–Fe(2)–C(15)	94.2 (1)	Fe(2)–C(1)–C(2)	161.1 (2)
Fe(2)–Fe(1)–C(11)	88.48 (8)	C(14)–Fe(2)–C(16)	96.0 (1)	Fe(3)–C(1)–C(2)	81.6 (1)
Fe(2)–Fe(1)–C(12)	89.64 (8)	C(15)–Fe(2)–C(16)	96.8 (1)	Fe(1)–C(2)–Fe(3)	87.82 (7)
Fe(2)–Fe(1)–C(13)	171.18 (8)	Fe(2)–Fe(3)–S	80.46 (2)	Fe(1)–C(2)–C(1)	65.2 (1)
S–Fe(1)–C(1)	87.42 (6)	Fe(2)–Fe(3)–C(1)	42.84 (6)	Fe(1)–C(2)–C(3)	132.5 (2)
S–Fe(1)–C(2)	86.26 (6)	Fe(2)–Fe(3)–C(2)	75.61 (6)	Fe(3)–C(2)–C(1)	65.0 (1)
S–Fe(1)–C(11)	84.98 (8)	Fe(2)–Fe(3)–C(17)	92.39 (9)	Fe(3)–C(2)–C(3)	132.5 (2)
S–Fe(1)–C(12)	169.29 (8)	Fe(2)–Fe(3)–C(18)	175.88 (8)	C(1)–C(2)–C(3)	146.1 (2)
S–Fe(1)–C(13)	97.64 (8)	Fe(2)–Fe(3)–C(19)	83.71 (8)	C(2)–C(3)–C(4)	112.9 (2)
C(1)–Fe(1)–C(2)	33.61 (8)	S–Fe(3)–C(1)	87.27 (6)	C(2)–C(3)–C(5)	108.5 (2)
C(1)–Fe(1)–C(11)	131.1 (1)	S–Fe(3)–C(2)	85.98 (6)	C(2)–C(3)–C(6)	108.2 (2)
C(1)–Fe(1)–C(12)	87.4 (1)	S–Fe(3)–C(17)	172.84 (9)	C(4)–C(3)–C(5)	108.0 (2)
C(1)–Fe(1)–C(13)	129.0 (1)	S–Fe(3)–C(18)	97.03 (9)	C(4)–C(3)–C(6)	109.6 (2)
C(2)–Fe(1)–C(11)	162.9 (1)	S–Fe(3)–C(19)	86.56 (8)	C(5)–C(3)–C(6)	109.6 (2)
C(2)–Fe(1)–C(12)	94.5 (1)	C(1)–Fe(3)–C(2)	33.45 (8)	S–C(7)–C(8)	115.7 (2)
C(2)–Fe(1)–C(13)	95.8 (1)	C(1)–Fe(3)–C(17)	87.4 (1)	S–C(7)–C(9)	105.1 (2)
C(11)–Fe(1)–C(12)	91.5 (1)	C(1)–Fe(3)–C(18)	134.2 (1)	S–C(7)–C(10)	105.8 (2)
C(11)–Fe(1)–C(13)	99.9 (1)	C(1)–Fe(3)–C(19)	126.4 (1)	C(8)–C(7)–C(9)	110.2 (2)
C(12)–Fe(1)–C(13)	92.9 (1)	C(2)–Fe(3)–C(17)	92.2 (1)	C(8)–C(7)–C(10)	110.2 (2)
Fe(1)–Fe(2)–Fe(3)	72.19 (1)	C(2)–Fe(3)–C(18)	101.0 (1)	C(9)–C(7)–C(10)	109.7 (2)
Fe(1)–Fe(2)–C(1)	50.79 (6)	C(2)–Fe(3)–C(19)	159.0 (1)	Fe(1)–C(11)–O(11)	177.3 (3)
Fe(1)–Fe(2)–C(14)	97.10 (8)	C(17)–Fe(3)–C(18)	90.1 (1)	Fe(1)–C(12)–O(12)	178.6 (3)
Fe(1)–Fe(2)–C(15)	158.75 (8)	C(17)–Fe(3)–C(19)	92.8 (1)	Fe(1)–C(13)–O(13)	176.6 (2)
Fe(1)–Fe(2)–C(16)	99.89 (8)	C(18)–Fe(3)–C(19)	99.4 (1)	Fe(2)–C(14)–O(14)	177.9 (2)
Fe(3)–Fe(2)–C(1)	51.28 (7)	Fe(1)–S–Fe(3)	86.29 (2)	Fe(2)–C(15)–O(15)	179.4 (2)
Fe(3)–Fe(2)–C(14)	158.88 (8)	Fe(1)–S–C(7)	119.28 (8)	Fe(2)–C(16)–O(16)	178.0 (2)
Fe(3)–Fe(2)–C(15)	91.12 (8)	Fe(3)–S–C(7)	119.23 (8)	Fe(3)–C(17)–O(17)	179.3 (3)
Fe(3)–Fe(2)–C(16)	103.70 (9)	Fe(1)–C(1)–Fe(2)	86.59 (9)	Fe(3)–C(18)–O(18)	174.5 (3)
C(1)–Fe(2)–C(14)	107.8 (1)	Fe(1)–C(1)–Fe(3)	98.25 (9)	Fe(3)–C(19)–O(19)	177.3 (2)

[a] Numbers in parentheses are estimated standard deviations in the least significant digits.

in 8 (1.867 (3)–2.059 (3) Å). In this structure the μ_3-acetylide group can clearly be regarded as a 5-electron donor so the open triangular cluster is as expected for a 50-electron species.

Carty has reported the synthesis and crystal structures of related phosphido- and acetylide-bridged triruthenium and triosmium clusters (eq 6).[6,11,12]

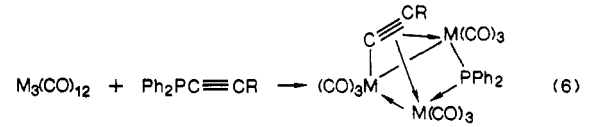

(6)

10

M = Ru, Os ; R = Ph, ^{i}Pr, ^{t}Bu

Although one can consider **9** as resulting from the formal insertion of an $Fe(CO)_3$ moiety into the electron-rich Fe–S bond of **5**, thereby appearing to be fundamentally different than **8**, the two complexes are in fact closely related. Transformation of **11** (the ^{t}Bu analogue of **8**) to **9** can readily occur by movement of the bridging thiolato group from Fe(2) to Fe(1) such that it bridges Fe(1) and Fe(3) instead of the Fe(2)–Fe(3) bond. This would be accompanied by the slight movement of Fe(3) closer to C(2) forming the interaction with a π bond of C(1)–C(2). This facile interconversion between **9** and **11** is confirmed by dissolving red crystals of **9** in pentane producing a deep red solution which over a period of 10–15 min becomes brownish green. TLC shows the presence of olive-green (likely **11**) and red (likely **9**) products. Apparently, an equilibrium is reached and complete conversion does not occur. However, when the solvent is removed in vacuo, only a red solid (**9**) remains.

The solubility and the equilibrium favoring either species of type **9** or **11** is, not surprisingly, influenced by the bulk of the acetylide substituent, so with R = Ph the unsymmetrical species **8** is the only one observed; the symmetrical isomer is not observed in solution. It thus appears that whether species of type **9** or **11** will be favored in either solution or the solid state is determined primarily by steric factors. Unfortunately, the equilibrium between **9** and **11** makes the ^{13}C NMR spectrum difficult to interpret. However, it does show the presence of at least three *tert*-butyl thiolate resonances (δ_C 30.83, 31.23, and 33.10) as well as four possible acetylide signals (δ_C 149.49, 202.40, 215.14, and 220.21), consistent with the presence of two isomers in solution. (The *tert*-butyl resonance at 33.10 ppm is considerably more intense than the other two and, therefore, may result from *two* chemically equivalent *tert*-butyl ligands.) Likely, the ^{13}C NMR signals at 149.49 and 215.14 ppm can be assigned to the acetylide carbon atoms of the red isomer **9** while the resonances at 202.40 and 220.21 ppm may be attributed to the corresponding green isomer of type **11** (which cannot be isolated and characterized in the solid state).

Somewhat surprisingly, $(\mu\text{-}\sigma,\pi\text{-}C{\equiv}CSiMe_3)(\mu\text{-}^t BuS)Fe_2(CO)_6$ (**1**) did not react with diiron nonacarbonyl at room temperature. When the reaction mixture was heated to reflux, only decomposition was observed. Further research into the utility of $(\mu\text{-}\sigma,\pi\text{-}C{\equiv}CR')(\mu\text{-}RS)Fe_2(CO)_6$, as general reagents for cluster synthesis is continuing.

Experimental Section

General Comments. All reactions were carried out under an atmosphere of prepurified tank nitrogen. Tetrahydrofuran (THF) was distilled under nitrogen from sodium/benzophenone ketyl and purged with nitrogen prior to use. *tert*-Butyl and phenyl mercaptans were purged with nitrogen and used without further purification. Phenylbromoacetylene (PhC≡CBr), (trimethylsilyl)bromoacetylene ($Me_3SiC{\equiv}CBr$), and *tert*-butylbromoacetylene ($^tBuC{\equiv}CBr$) all were prepared by a literature procedure[13] and purged with nitrogen prior to use. Diiron nonacarbonyl ($Fe_2(CO)_9$)[14] and triiron dodecacarbonyl ($Fe_3(CO)_{12}$)[15] were also prepared by literature methods. Dicobalt octacarbonyl was purchased from Strem Chemical Co. and was used as received.

The progress of all reactions was monitored by thin-layer chromatography (Baker Flex—Silica Gel 1B-F). Purification by filtration chromatography in which the reaction products were dissolved in a suitable solvent and chromatographed on a bed of EM Science, or Sigma 100-300 mesh silicic acid (ca. 200 mL) in a 350-mL glass-fritted filter funnel was used in most cases. Further purification by medium-pressure column chromatography was accomplished with a 300 × 25 mm column using Sigma 230–400 mesh silica gel. Column chromatography under nitrogen was accomplished with a 200 × 25 mm gravity column (solvent reservoir at the top) using Sigma 230–400 mesh silica gel (dried for several hours at ~150 °C in vacuo). All chromatography was completed without exclusion of atmospheric moisture or oxygen except where specified. Solid products were recrystallized from deoxygenated solvents at −20 °C.

Solution infrared spectra (NaCl windows) were obtained by using a Perkin-Elmer Model 1430 double-beam grating infrared spectrophotometer. Proton NMR spectra were recorded on either a JEOL FX-90Q, a Bruker WM-250, or a Varian XL-300 NMR spectrometer operating at 90, 250, or 300 MHz, respectively. Carbon-13 NMR spectra were obtained by using a Bruker WH-270, a Varian XL-300, or a Varian XL-400 spectrometer operating at 67.9, 75.4, or 100.5 MHz, respectively. Electron-impact mass spectra were obtained by using a Finnigan-3200 mass spectrometer operating at 70 eV. Field desorption mass spectra were obtained by using a Finnigan MAT-731 mass spectrometer operating in the positive ion mode. Masses were correlated by using the following isotopes: ^1H, ^{12}C, ^{14}N, ^{16}O, ^{28}Si, ^{32}S, ^{56}Fe, and ^{59}Co. Melting points were determined in air on a Büchi melting point apparatus using analytically pure samples and are uncorrected. Microanalyses were performed by Scandinavian Microanalytical Laboratory, Herlev, Denmark.

X-ray Data Collection for 2 and 4. Crystal, data collection, and refinement parameters are collected in Table IX. Black crystals of **2** and deep red crystals of **4** were grown from pentane and mounted on glass fibers with epoxy cement. The unit-cell parameters for **2** and **4** were obtained from the least-squares fit of 25 reflections ($22° \leq 2\theta \leq 25°$). Both data collections were at ambient temperatures (23 ± 1 °C). Preliminary photographic characterization showed $\bar{1}$ and $2/m$ Laue symmetry for **2** and **4**, respectively. TRACER failed to find higher symmetries for either. For **2**, the centrosymmetric alternative, $P\bar{1}$, was suggested by E statistics and confirmed by the chemically sensible results of refinement. Systematic absences in the diffraction data ($h0l$, $l = 2n + 1$; $0k0$, $k = 2n + 1$) uniquely established the space group for **4**. Three standard reflections monitored every 197 data showed insignificant variation. Empirical corrections for absorption were applied to both data sets (216 Ψ-scan reflections, pseudoellipsoid model).

Structure Solution and Refinement for 2 and 4. Both **2** and **4** were solved by direct methods to locate the metal atoms. The remaining non-hydrogen atoms were located from subsequent difference Fourier syntheses. All hydrogen atoms were included as idealized isotropic contributions (d(CH) = 0.96 Å; $U = 1.2U$ for attached C). The phenyl ring in **4** was treated as a rigid, planar hexagon (d(CC) = 1.395 Å). All non-hydrogen atoms were refined with anisotropic thermal parameters. Atomic coordinates for **2** and **4** are given in Tables XI and XII. All computer programs and the sources of the scattering factors are contained in the SHELXTL program library (5.1) (Nicolet Corp., Madison, WI).

(11) Carty, A. J. *Adv. Chem. Ser.* **1981**, *No. 196*, 163.
(12) Carty, A. J.; Taylor, N. J.; Smith, W. F. *J. Chem. Soc., Chem. Commun.* **1979**, 750.
(13) *Synthesis of Acetylenes, Allenes, and Cumulenes*; Brandsma, L., Verkruijsse, H. D., Eds.; Elsevier: New York, 1981; p 98.
(14) *Organometallic Synthesis*: King, R. B., Ed.; Academic: New York, 1965; Vol. 1, p 93.
(15) McFarlane, W.; Wilkinson, G. *Inorg. Synth.* **1966**, *8*, 181.

Table IX. Summary of Crystal Data and Details of Intensity Collection for Compounds 2 and 4

	$CoFe_2(CO)_9$-(CCSiMe$_3$) (2)	$Co_2Fe_2(CO)_{11}$(S^{t}Bu)-(CCPh) (4)
fw	519.91	727.95
space group	$P\bar{1}$ (No. 2)	$P2_1/c$ (No. 14)
a, Å	9.046 (2)	14.303 (4)
b, Å	9.509 (2)	11.710 (3)
c, Å	11.721 (3)	16.462 (4)
α, deg	101.41 (2)	
β, deg	97.58 (2)	97.86 (2)
γ, deg	90.64 (2)	
V, Å^3	978.8 (2)	2731 (1)
Z	2	4
ρ_{calcd}, g/cm^3	1.764	1.771
radiatn	Mo Kα (λ = 0.710 73 Å), graphite monochromated	
2θ limit, deg	50	50
abs coeff μ, cm^{-1}	24.00	23.74
scan type	Wyckoff	Wyckoff
unique data collected	3459	4781
unique data used ($F_o \geq 5\sigma(F_o)$)	2772 ($\pm h,\pm k,+l$)	3299 ($\pm h,k,l$)
cryst dimens, mm	0.31 × 0.32 × 0.36	0.20 × 0.36 × 0.40
transmissn range	0.317–0.248	0.329–0.232
no. of parameters varied	245	340
GOF	1.289	1.288
$R(F)$	0.036	0.046
$R(wF)$	0.042	0.049
$\Delta(\rho)$, e Å^{-3}	0.51	0.63

X-ray Data Collection for 8 and 9. Suitable quality, approximately spherical, green-black crystals of 8 and irregularly shaped red-brown crystals of 9 were grown from pentane. Both were mounted in air on glass fibers by using epoxy resin, and 9 was further coated with epoxy to prevent further exposure to air. Unit cell parameters were obtained from a least-squares analysis of 25 reflections in the range 20.2° ≤ 2θ ≤ 25.8° (8) and 22.0° ≤ 2θ ≤ 25.9° (9), which were accurately centered (in both positive and negative θ) at 22 °C on an Enraf-Nonius CAD4 diffractometer, using Mo Kα radiation. The systematic absences for 8 ($0kl$, $k = 2n + 1$; $h0l$, $l = 2n + 1$; $hk0$, $h = 2n + 1$) and 9 ($h0l$, $l = 2n + 1$; $0k0$, $k = 2n + 1$) unambiguously established the space groups as $Pbca$ and $P2_1/c$ for the orthorhombic and monoclinic crystals, respectively. Intensity data were collected at 22 °C with the diffractometer in the bisecting mode using a $\theta/2\theta$ scan technique as indicated in Table X. The intensities of three standard reflections were measured every 1 h for each data set to assess possible crystal decomposition or movement, but since there was no significant variation in either set, no correction was applied. Data were processed in the usual manner by using a value of 0.04 for the ignorance factor (p).[16]

Structure Solution and Refinement. Both structures were solved by using MULTAN 82[17] to locate the Fe and S atoms. Subsequent full-matrix, least-squares cycles and difference Fourier calculations led to the location of all additional atoms. Atomic scattering factors for hydrogen[18] and the other atoms[19] were taken from the usual tabulations, and anomalous dispersion terms[20] for all atoms were included in the calculation of F_c. All hydrogens were located but were input to the least-squares cycles in their idealized positions, obtained by assuming the appropriate hybridization of the attached carbon atom and using a C–H distance of 0.95 Å. The hydrogen atoms were not refined but were allowed to "ride" on their attached carbon atoms and were assigned isotropic thermal parameters of 20% larger than their attached carbon atom. All other atoms were refined anisotropically. Absorption corrections were applied to both data sets by using the method of Walker and Stuart.[21] Refinement details are given in Table X. On the final difference Fourier maps the highest residuals measured 0.23 e Å^{-3} (8) and 0.22 e Å^{-3} (9) and can be

Table X. Summary of Crystal Data and Details of Intensity Collection for Compounds 8 and 9

	$Fe_3(CO)_9$(S^{t}Bu)-(CCPh) (8)	$Fe_3(CO)_9$(S^{t}Bu)-(CC^{t}Bu) (9)
fw	609.95	589.95
space group	$Pbca$ (No. 61)	$P2_1/c$ (No. 14)
a, Å	14.413 (2)	10.000 (1)
b, Å	23.269 (2)	14.953 (2)
c, Å	14.551 (1)	16.299 (1)
β, deg		102.364 (7)
V, Å^3	4880.0	2380.7
Z	8	4
ρ_{calcd}, g/cm^3	1.660	1.646
radiatn	Mo Kα [$\lambda(\bar{\alpha})$ = 0.710 69 Å], graphite monochromated	
detector aperture, mm	4 × (3.00 + 1.00 tan θ)	
2θ limit, deg	1.0 ≤ 2θ ≤ 52.0	1.0 ≤ 2θ ≤ 55.0
scan type	$\theta/2\theta$	$\theta/2\theta$
scan width, deg	(0.60 + 0.347 tan θ) in θ	
bkgd	25% on low- and high-angle sides	
unique data collected	4753	5340
unique data used ($F_o^2 \geq 3\sigma(F_o^2)$)	3224 (h,k,l)	3816 ($h,k,\pm l$)
abs coeff μ, cm^{-1}	18.885	19.323
cryst dimens, mm	0.38 × 0.38 × 0.38	0.41 × 0.57 × 0.44
range in absorptn correctn factors	0.839–1.053	0.893–1.100
final no. of parameters varied	307	289
error in obsvn unit weight	1.054	1.151
R	0.024	0.027
R_w	0.030	0.035

Table XI. Atomic Coordinates (×10^4) and Isotropic Thermal Parameters (Å^2 × 10^3) for 2

	x	y	z	U^a
Fe(1)	7303.8 (6)	3819.5 (6)	3157.6 (5)	36.3 (2)
Fe(2)	8876.4 (6)	1699.8 (6)	2687.2 (5)	36.5 (2)
Co	6593.9 (6)	1444.3 (7)	3818.6 (5)	43.6 (2)
Si	6754 (1)	2426 (1)	−58 (1)	46 (1)
O(1)	8455 (4)	4830 (4)	5629 (3)	72 (2)
O(2)	4466 (5)	5290 (5)	3127 (5)	97 (2)
O(3)	9053 (5)	5967 (4)	2362 (4)	81 (2)
O(4)	11253 (4)	3019 (5)	1725 (4)	79 (2)
O(5)	9186 (5)	−1292 (4)	1513 (5)	106 (2)
O(6)	10562 (4)	1730 (5)	4991 (3)	84 (2)
O(7)	6244 (5)	−1681 (4)	3331 (4)	80 (2)
O(8)	7660 (5)	1750 (5)	6342 (3)	85 (2)
O(9)	3493 (4)	2091 (6)	4019 (4)	99 (2)
C(1)	7980 (5)	4381 (5)	4675 (4)	51 (2)
C(2)	5553 (5)	4716 (5)	3134 (5)	59 (2)
C(3)	8367 (5)	5129 (5)	2639 (4)	51 (2)
C(4)	10337 (5)	2524 (5)	2093 (4)	50 (2)
C(5)	9099 (5)	−129 (5)	1993 (5)	60 (2)
C(6)	9864 (5)	1721 (6)	4110 (4)	55 (2)
C(7)	6393 (5)	−474 (6)	3534 (4)	54 (2)
C(8)	7273 (5)	1654 (5)	5382 (4)	51 (2)
C(9)	4691 (5)	1842 (6)	3980 (4)	58 (2)
C(10)	4772 (6)	2919 (7)	−314 (5)	79 (3)
C(11)	8027 (6)	3757 (6)	−414 (4)	64 (2)
C(12)	7034 (7)	597 (6)	−892 (5)	76 (2)
C(13)	7103 (4)	2328 (4)	1525 (4)	39 (1)
C(14)	6645 (4)	1798 (4)	2352 (4)	37 (1)

[a] Equivalent isotropic U defined as one-third of the trace of the orthogonalized U_{ij} tensor.

(16) Doedens, R. J.; Ibers, J. A. *Inorg. Chem.* **1968**, *6*, 204.
(17) Main, P.; Lessinger, L.; Woofson, M. M.; Germain, G.; Declercq, J. P., MULTAN 11/82, *A System of Computer Programs for the Automatic Solution of Crystal Structures from X-ray Diffraction Data*; University of York, York, England, and University of Louvain, Louvain, Belgium.
(18) Stewart, R. F.; Davidson, E. F.; Simpson, W. T. *J. Chem. Phys.* **1965**, *42*, 3175.
(19) Cromer, D. T.; Waber, J. T. *International Tables for X-ray Crystallography*; Kynoch: Birmingham, England, 1974; Vol. IV, Table 2.2A.
(20) Cromer, D. T.; Liberman, D. *J. Chem. Phys.* **1970**, *53*, 1891.
(21) Walker, N.; Stuart, D. *Acta Crystallogr., Sect. A: Found. Crystallogr.* **1983**, *A39*, 1581.

Table XII. Atomic Coordinates (×10⁴) and Isotropic Thermal Parameters (Å² × 10³) for 4

	x	y	z	U[a]
Co(1)	3968.8 (5)	5552.6 (7)	6871.2 (4)	39.9 (3)
Co(2)	3061.0 (5)	5606.6 (7)	5477.1 (4)	41.9 (3)
Fe(1)	3327.6 (5)	7522.5 (6)	6326.3 (5)	34.3 (2)
Fe(2)	1674.3 (6)	7618.2 (7)	6669.8 (5)	46.0 (3)
S	2175 (1)	8426 (1)	5544 (1)	40 (1)
C(1)	4230 (4)	4050 (5)	6946 (4)	50 (2)
O(1)	4373 (3)	3107 (4)	6975 (3)	68 (2)
C(2)	4088 (4)	5940 (5)	7936 (4)	50 (2)
O(2)	4188 (4)	6205 (4)	8608 (3)	79 (2)
C(3)	5126 (4)	6002 (5)	6670 (4)	52 (2)
O(3)	5860 (3)	6229 (4)	6549 (3)	72 (2)
C(4)	3115 (4)	4125 (5)	5205 (4)	54 (2)
O(4)	3115 (4)	3197 (4)	5038 (3)	89 (2)
C(5)	4019 (5)	6136 (5)	4985 (3)	49 (2)
O(5)	4628 (3)	6415 (4)	4650 (3)	75 (2)
C(6)	2122 (5)	5968 (6)	4674 (4)	60 (2)
O(6)	1549 (4)	6153 (5)	4154 (3)	98 (2)
C(7)	4380 (4)	8186 (5)	6080 (4)	56 (2)
O(7)	5035 (4)	8628 (4)	5927 (4)	100 (3)
C(8)	3246 (5)	8259 (5)	7294 (4)	61 (3)
O(8)	3451 (3)	8724 (4)	7885 (3)	69 (2)
C(9)	1147 (5)	8878 (5)	7038 (4)	56 (2)
O(9)	761 (4)	9621 (4)	7286 (3)	88 (2)
C(10)	615 (5)	7006 (6)	6086 (4)	55 (2)
O(10)	−37 (4)	6621 (5)	5723 (4)	97 (3)
C(11)	1567 (4)	6873 (5)	7610 (4)	54 (2)
O(11)	1496 (4)	6401 (4)	8190 (3)	80 (2)
C(12)	2593 (4)	5168 (5)	6559 (3)	38 (2)
C(13)	2487 (4)	6279 (4)	6434 (3)	38 (2)
C(14)	2278 (4)	10026 (5)	5491 (4)	48 (2)
C(15)	2898 (5)	10205 (5)	4807 (4)	66 (3)
C(16)	2730 (5)	10586 (5)	6273 (4)	64 (3)
C(17)	1276 (5)	10455 (6)	5208 (4)	71 (3)
C(21)	1228 (3)	3846 (3)	6277 (2)	52 (2)
C(22)	673	2962	6517	64 (3)
C(23)	908	2447	7282	66 (3)
C(24)	1699	2817	7807	64 (3)
C(25)	2255	3701	7567	54 (2)
C(26)	2019	4215	6802	42 (2)

[a] Equivalent isotropic U defined as one-third of the trace of the orthogonalized U_{ij} tensor.

compared to the intensities of carbon atoms on earlier maps of between 2.6 and 7.2 e Å^{-3} (**8**) and 4.2–7.2 e Å^{-3} (**9**).

The positional parameters and the equivalent isotropic B's of the non-hydrogen atoms are given in Table XIII for **8** and Table XIV for **9**. Additional information is available as supplementary material.[22]

The computer programs used for compounds **8** and **9** include the Enraf-Nonius Structure Determination Package by B.A. Frenz (Computing in Crystallography; Delft University Press: Delft, Holland, 1978; pp 67–71) and several locally written or modified programs.

Reaction of (μ-σ,π-C≡CSiMe$_3$)(μ-^{t}BuS)Fe$_2$(CO)$_6$ with Co$_2$(CO)$_8$. A 100-mL round-bottomed flask equipped with a stir bar and rubber septum was charged with 0.68 g (1.46 mmol) of (μ-σ,π-C≡CSiMe$_3$)(μ-^{t}BuS)Fe$_2$(CO)$_6$ (**1**), degassed by three evacuation/nitrogen-backfill cycles, and charged with 10 mL of THF by syringe. To the resulting red solution was added, by cannula at room temperature, a THF solution (15 mL) containing 1.01 g (2.95 mmol) of dicobalt octacarbonyl. After the reaction mixture had been stirred for 72 h at room temperature, the solvent was removed in vacuo and the resulting dark oil was purified by filtration chromatography. Hexane eluted a purplish red band which gave 0.66 g (1.26 mmol, 87%) of (μ_3,η^2-C≡CSiMe$_3$)-CoFe$_2$(CO)$_9$ (**2**) as an air-stable, black solid, mp 116.0–117.0 °C after recrystallization from pentane.

Anal. Calcd for C$_{14}$H$_9$CoFe$_2$O$_9$Si: C, 32.34; H, 1.74. Found: C, 32.23; H, 1.74. IR (CCl$_4$): 1663 s (C≡C); terminal carbonyl region (pentane) 2095 w, 2055 vs, 2045 vs, 2020 s, 2005 m, 1985 w cm^{-1}. ^{1}H NMR (CDCl$_3$, 300 MHz): δ 0.47 (s, Si(CH$_3$)$_3$). ^{13}C NMR (CDCl$_3$, 100.5 MHz): δ 1.05 (q, J = 120.8 Hz, Si(CH$_3$)$_3$), 97.43 (s, C≡CSiMe$_3$), 202.60 (s, C≡CSiMe$_3$), 209.35 and 211.34 (both s, CO). Mass spectrum (EI): m/z (relative intensity) 520 (M$^+$, 12), 492 (M$^+$ − CO, 13), 464 (M$^+$ − 2CO, 14), 436 (M$^+$ − 3CO,

(22) See paragraph at end of paper regarding supplementary material.

Table XIII. Positional Parameters and Isotropic B's for Compound 8

atom	x	y	z	B, Å²
Fe(1)	0.1173 (3)	0.12952 (2)	−0.13306 (2)	2.941 (7)
Fe(2)	0.21937 (2)	0.05855 (1)	−0.02691 (2)	2.659 (7)
Fe(3)	0.20716 (3)	0.12053 (2)	0.11616 (2)	2.684 (7)
S	0.31141 (4)	0.13627 (3)	0.00412 (5)	2.77 (1)
O(13)	0.2923 (2)	0.1573 (1)	−0.2310 (2)	6.31 (6)
O(14)	0.0510 (2)	0.04229 (9)	−0.2612 (2)	6.20 (6)
O(15)	0.0069 (2)	0.21781 (9)	−0.2230 (2)	5.49 (5)
O(16)	0.3328 (2)	0.0162 (1)	−0.1800 (2)	6.80 (6)
O(17)	0.2804 (2)	−0.0258 (1)	0.1089 (2)	6.57 (6)
O(18)	0.0676 (1)	−0.02219 (9)	−0.0627 (2)	4.70 (5)
O(19)	0.3266 (2)	0.0814 (1)	0.2695 (2)	5.87 (6)
O(20)	0.1862 (2)	0.2403 (1)	0.1699 (2)	7.34 (7)
O(21)	0.0459 (1)	0.0780 (1)	0.2174 (2)	5.49 (5)
C(1)	0.1279 (2)	0.1207 (1)	0.0073 (2)	2.69 (5)
C(2)	0.0457 (2)	0.1348 (1)	−0.0264 (2)	2.73 (5)
C(3)	−0.0447 (2)	0.1567 (1)	0.0041 (2)	3.01 (5)
C(4)	−0.0541 (2)	0.1866 (1)	0.0867 (2)	3.97 (6)
C(5)	−0.1395 (2)	0.2075 (1)	0.1134 (3)	5.05 (8)
C(6)	−0.2163 (2)	0.1977 (2)	0.0610 (3)	5.93 (9)
C(7)	−0.2086 (2)	0.1676 (2)	−0.0203 (3)	5.79 (9)
C(8)	−0.1225 (2)	0.1475 (1)	−0.0491 (2)	4.42 (7)
C(9)	0.4377 (2)	0.1264 (1)	0.0275 (2)	3.62 (6)
C(10)	0.4646 (2)	0.1734 (1)	0.0956 (2)	4.94 (7)
C(11)	0.4637 (2)	0.0671 (1)	0.0626 (3)	4.91 (7)
C(12)	0.4832 (2)	0.1379 (2)	−0.0662 (2)	6.01 (9)
C(13)	0.2272 (2)	0.1461 (1)	−0.1907 (2)	4.20 (7)
C(14)	0.0790 (2)	0.0765 (1)	−0.2133 (2)	3.87 (6)
C(15)	0.0508 (2)	0.1836 (1)	−0.1880 (2)	3.69 (6)
C(16)	0.2885 (2)	0.0330 (1)	−0.1214 (2)	3.96 (6)
C(17)	0.2599 (2)	0.0100 (1)	0.0598 (2)	4.13 (6)
C(18)	0.1256 (2)	0.0100 (1)	−0.0486 (2)	3.29 (6)
C(19)	0.2848 (2)	0.0961 (1)	0.2081 (2)	3.73 (6)
C(20)	0.1952 (2)	0.1939 (1)	0.1495 (2)	4.05 (6)
C(21)	0.1085 (2)	0.0942 (1)	0.1781 (2)	3.52 (6)

Table XIV. Positional Parameters and Isotroic B's for Compound 9

atom	x	y	z	B, Å²
Fe(1)	0.80785 (3)	0.09773 (2)	0.24412 (2)	2.716 (6)
Fe(2)	0.61925 (3)	0.04222 (2)	0.32857 (2)	2.854 (6)
Fe(3)	0.70880 (3)	−0.10166 (2)	0.25835 (2)	2.800 (6)
S	0.68729 (5)	−0.00225 (4)	0.14745 (3)	2.71 (1)
O(11)	0.6113 (2)	0.2292 (1)	0.1560 (1)	6.02 (5)
O(12)	0.9129 (2)	0.2248 (1)	0.3800 (1)	5.71 (5)
O(13)	1.0340 (2)	0.1359 (2)	0.1609 (1)	5.50 (5)
O(14)	0.6253 (2)	0.1986 (1)	0.4373 (1)	6.16 (5)
O(15)	0.4882 (2)	−0.0718 (2)	0.4341 (1)	6.19 (5)
O(16)	0.3662 (2)	0.0939 (2)	0.2097 (1)	7.10 (7)
O(17)	0.7260 (2)	−0.2092 (2)	0.4106 (1)	6.54 (6)
O(18)	0.8140 (2)	−0.2547 (1)	0.1806 (1)	6.44 (5)
O(19)	0.4169 (2)	−0.1408 (2)	0.1962 (1)	5.52 (5)
C(1)	0.7950 (2)	0.0037 (2)	0.3370 (1)	2.73 (4)
C(2)	0.9037 (2)	−0.0246 (2)	0.3167 (1)	2.86 (4)
C(3)	1.0513 (2)	−0.0537 (2)	0.3479 (2)	3.52 (5)
C(4)	1.1197 (3)	−0.0824 (2)	0.2771 (2)	5.17 (7)
C(5)	1.0534 (3)	−0.1332 (2)	0.4068 (2)	5.79 (8)
C(6)	1.1306 (3)	0.0244 (2)	0.3960 (2)	5.87 (8)
C(7)	0.7567 (2)	−0.0337 (2)	0.0536 (1)	3.48 (5)
C(8)	0.9029 (2)	−0.0696 (2)	0.0722 (2)	4.14 (6)
C(9)	0.6577 (3)	−0.1045 (2)	0.0077 (2)	5.16 (7)
C(10)	0.7473 (3)	0.0507 (2)	−0.0000 (2)	4.79 (6)
C(11)	0.6865 (3)	0.1787 (2)	0.1919 (2)	3.81 (6)
C(12)	0.8738 (3)	0.1751 (2)	0.3278 (2)	3.80 (5)
C(13)	0.9466 (3)	0.1186 (2)	0.1922 (2)	3.73 (5)
C(14)	0.6244 (3)	0.1388 (2)	0.3943 (2)	3.84 (5)
C(15)	0.5397 (3)	−0.0268 (2)	0.3931 (2)	3.90 (5)
C(16)	0.4647 (2)	0.0732 (2)	0.2545 (2)	4.23 (6)
C(17)	0.7184 (3)	−0.1676 (2)	0.3516 (2)	4.19 (6)
C(18)	0.7780 (3)	−0.1928 (2)	0.2096 (2)	4.05 (6)
C(19)	0.5295 (3)	−0.1240 (2)	0.2216 (2)	3.78 (5)

26), 408 (M^+ – 4CO, 15), 380 (M^+ – 5CO, 100), 352 (M^+ – 6CO, 46), 324 (M^+ – 7CO, 39), 296 (M^+ – 8CO, 33), 268 (M^+ – 9CO, 75), 212 ($FeCoC{\equiv}CSiMe_3$, 12), 156 ($CoC{\equiv}CSiMe_3$, 8), 115 (FeCo, 4), 97 ($C{\equiv}CSiMe_3$, 4), 73 ($SiMe_3$, 12), 59 (Co, 19), 56 (Fe, 4). Hexane/CH_2Cl_2 then eluted a minor dark purple band which was not collected.

Reaction of (μ-σ,π-C≡CPh)(μ-^{t}BuS)$Fe_2(CO)_6$ with $Co_2(CO)_8$. In an experiment similar to the reaction of 1 with dicobalt octacarbonyl, a THF solution containing 0.68 g (1.45 mmol) of (μ-σ,π-C≡CPh)(μ-^{t}BuS)$Fe_2(CO)_6$ (**3**) and 1.03 g (3.01 mmol) of dicobalt octacarbonyl was stirred for 22 h at room temperature. Removal of the solvent in vacuo left a black oil which was purified by filtration chromatography. Hexane eluted a brown-red band which was unstable in air and was not collected. Hexane/CH_2Cl_2 (7/1 v/v) eluted a purplish black band which gave 0.72 g (0.98 mmol, 68%) of (μ_4-C≡CPh)(μ-^{t}BuS)(μ-CO)$Co_2Fe_2(CO)_{10}$ (**4**) (a mixture of two inseparable isomers), as an air-stable, black solid, mp 118 °C dec after recrystallization from pentane/CH_2Cl_2.

Anal. Calcd for $C_{23}H_{14}Co_2Fe_2O_{11}S$: C, 37.95; H, 1.94. Found: C, 38.07; H, 2.06. IR (CCl_4): 1850 vs (μ-CO), 1620 m (C≡C); carbonyl region (pentane) 2090 w, 2060 s, 2040 vs, 2025 s, 2015 s, 2010 w, 2000 w, 1995 w, 1985 w, 1885 w (μ-CO) cm^{-1}. ^1H NMR (CD_2Cl_2, 250 MHz): δ 1.53 (s, 9 H, $SC(CH_3)_3$ major isomer), 1.56 (s, 9 H, $SC(CH_3)_3$ minor isomer), 7.46–7.75 (m, 10 H, C_6H_5 both isomers). Major/minor ratio = 1.7/1.0. ^{13}C NMR (CD_2Cl_2, 75.4 MHz): δ 33.25 (q, J = 127.0 Hz, $SC(CH_3)_3$ both isomers), 47.92 (s, $SC(CH_3)_3$ major isomer), 48.05 (s, $SC(CH_3)_3$ minor isomer), 127.71–131.62 (m, C_6H_5), 133.60 (s, ipso C_6H_5), 139.23, 144.27, 148.63, and 152.21 (all s, alkynyl C), 200.38, 206.10, 208.75, 210.59, 211.19, and 219.50 (all s, CO), 232.84 (s, μ-CO). Mass spectrum (FD): m/z (relative intensity): 727 (M^+ – H).

Reaction of (μ-σ,π-C≡C^{t}Bu)(μ-^{t}BuS)$Fe_2(CO)_6$ with $Co_2(CO)_8$. In an experiment similar to the reaction of 1 with dicobalt octacarbonyl, a THF solution containing 0.68 g (1.51 mmol) of (μ-σ,π-C≡C^{t}Bu)(μ-^{t}BuS)$Fe_2(CO)_6$ (**5**) and 1.06 g (3.10 mmol) of dicobalt octacarbonyl was stirred for 72 h at room temperature. Removal of the solvent in vacuo left a dark oil which was purified by filtration chromatography. Hexane eluted a purplish red band which gave 0.95 g of a purple-red solid identified by its ^1H NMR and mass spectra to be a mixture of (μ_3-S)$Co_2Fe(CO)_9$ and (μ_3,η^2-C≡C^{t}Bu)$CoFe_2(CO)_9$ (**6**). Fractional recrystallization from pentane/CH_2Cl_2 yielded 0.33 g (0.67 mmol, 44%) of analytically pure (μ_3,η^2-C≡C^{t}Bu)$CoFe_2(CO)_9$ as an air-stable, black solid, mp 156.0–157.0 °C.

Anal. Calcd for $C_{15}H_9CoFe_2O_9$: C, 35.75; H, 1.80. Found: C, 35.91; H, 1.90. IR (CCl_4): 1680 w (C≡C); terminal carbonyl region (pentane) 2090 s, 2050 vs, 2040 vs, 2020 vs, 2000 s, 1980 s cm^{-1}. ^1H NMR ($CDCl_3$, 300 MHz): δ 1.56 (s, $C(CH_3)_3$). ^{13}C NMR ($CDCl_3$, 100.5 MHz): δ 33.80 (q, J = 126.6 Hz, $C(CH_3)_3$), 36.83 (s, $C(CH_3)_3$), 130.15 (s, C≡C^{t}Bu), 184.11 (s, C≡C^{t}Bu), 209.51 and 211.47 (both s, CO). Mass spectrum (EI): m/z (relative intensity) 504 (M^+, 15), 476 (M^+ – CO, 13), 448 (M^+ – 2CO, 10), 420 (M^+ – 3CO, 25), 392 (M^+ – 4CO, 19), 364 (M^+ – 5CO, 100), 336 (M^+ – 6CO, 44), 308 (M^+ – 7CO, 39), 280 (M^+ – 8CO, 35), 252 (M^+ – 9CO, 65), 196 ($Fe_2CoC{\equiv}CH$, 17), 140 ($CoFeC{\equiv}CH$, 19), 115 (FeCo, 14), 112 (Fe_2, 5), 56 (Fe, 8).

Pentane/CH_2Cl_2 (5/1 v/v) then eluted a purple-black band which gave 0.32 g (0.45 mmol, 30%) of (μ_4-C≡C^{t}Bu)(μ-^{t}BuS)(μ-CO)$Co_2Fe_2(CO)_{10}$ (**7**) as an air-stable, black solid, mp 108.0–123.0 °C dec after recrystallization from pentane.

Anal. Calcd for $C_{21}H_{18}Co_2Fe_2O_{11}S$: C, 35.63; H, 2.56. Found: C, 35.77; H, 2.67. IR (CCl_4): 1843 vs (μ-CO); terminal carbonyl region (pentane) 2080 vw, 2055 vs, 2035 vs, 2020 vs, 2010 sh, 2002 w, 1978 w, and 1847 w (μ-CO) cm^{-1}. ^1H NMR (CD_2Cl_2, 300 MHz): δ 1.49 (s, $C(CH_3)_3$, 9 H minor isomer), 1.56 (s, 9 H, $C(CH_3)_3$ major isomer), 1.64 (s, 9 H, $C(CH_3)_3$ minor isomer), 1.72 (s, 9 H, $C(CH_3)_3$ major isomer). Major/minor ratio = 19.0/1.0. ^{13}C NMR (CD_2Cl_2, 67.9 MHz): δ 33.15 (q, J = 127.1 Hz, $C(CH_3)_3$), 33.82 (q, J = 121.1 Hz, $C(CH_3)_3$), 39.22 (s, $C(CH_3)_3$), 48.36 (s, $SC(CH_3)_3$), 148.22 and 151.20 (s, alkynyl C), 202.80, 206.73, 209.25, and 211.78 (all s, CO), 233.21 (s, μ-CO). Mass spectrum (EI): m/z (relative intensity) 708 (M^+, 1), 680 (M^+ – CO, 10), 652 (M^+ – 2CO, 22), 624 (M^+ – 3CO, 19), 596 (M^+ – 4CO, 17), 568 (M^+ – 5CO, 21), 540 (M^+ – 6CO, 37), 512 (M^+ – 7CO, 70), 484 (M^+ – 8CO, 41), 456 (M^+ – 9CO, 21), 428 (M^+ – 10CO, 11), 400 (M^+ – 11CO, 37), 344 ($HSFe_2Co_2C{\equiv}C^tBu$, 53), 288 ($HSFe_2Co_2C{\equiv}CH$, 12), 343 ($SFe_2Co_2C{\equiv}C^tBu$, 11), 287 ($SFe_2Co_2C{\equiv}CH$, 13), 81 (C≡C^{t}Bu, 12), 57 (^{t}Bu, 80), 56 (Fe, 57).

Reaction of (μ-σ,π-C≡CPh)(μ-^{t}BuS)$Fe_2(CO)_6$ with $Fe_2(CO)_9$. A 100-mL round-bottomed flask equipped with a stir bar and rubber septum was charged with 0.81 g (1.73 mmol) of (μ-σ,π-C≡CPh)(μ-^{t}BuS)$Fe_2(CO)_6$ (**3**) and 1.27 g (3.49 mmol) of diiron nonacarbonyl and then degassed by three evacuation/nitrogen-backfill cycles. Subsequently, 30 mL of toluene was added by syringe. An immediate reaction ensued with slow gas evolution and a gradual color change to brown-green. After the reaction mixture had been stirred for 40 h at room temperature, the solvent was removed in vacuo and the resulting dark oil was purified by column chromatography (gravity column) under nitrogen. Hexane eluted a dark green band which gave 0.96 g (1.57 mmol, 91%) of (μ_3-C≡CPh)(μ-^{t}BuS)$Fe_3(CO)_9$ (**8**) as a *dark green*, air-stable, solid, mp 88.0–92.0 °C after recrystallization from pentane.

Anal. Calcd for $C_{21}H_{14}Fe_3O_9S$: C, 41.35; H, 2.31. Found: C, 41.36; H, 2.42. IR (terminal carbonyl region (pentane)): 2070 m, 2040 vs, 2025 vs, 2005 vs, 1995 vs, 1978 s, 1970 m cm^{-1}. ^1H NMR (CD_2Cl_2, 300 MHz): δ 1.27 (s, 9 H, $SC(CH_3)_3$ minor isomer), 1.58 (s, 9 H, $SC(CH_3)_3$ major isomer), 7.63–8.12 (m, 10 H, C_6H_5 both isomers). Major/minor ratio = 8.0/1.0. ^{13}C NMR (CD_2Cl_2; 67.9 MHz): δ 32.76 (q, J = 127.8 Hz, $SC(CH_3)_3$ major isomer), 33.20 (q, J = 127.5 Hz, $SC(CH_3)_3$ minor isomer), 49.32 (s, $SC(CH_3)_3$), 127.33–133.22 (m, C_6H_5), 139.23 (s, ipso C_6H_5), 201.24 (s, $Fe_3C{\equiv}CPh$), 211.38 (s, Fe-CO), 228.61 (s, $Fe_3C{\equiv}CPh$). Mass spectrum (EI): m/z (relative intensity) 610 (M^+, 1), 582 (M^+ – CO, 7), 554 (M^+ – 2CO, 21), 526 (M^+ – 3CO, 4), 498 (M^+ – 4CO, 18), 470 (M^+ – 5CO, 43), 442 (M^+ – 6CO, 12), 414 (M^+ – 7CO, 37), 386 (M^+ – 8CO, 55), 358 (M^+ – 9CO, 16), 302 ($HSFe_3C{\equiv}CPh$, 100), 301 ($SFe_3C{\equiv}CPh$, 25), 246 ($HSFe_2C{\equiv}CPh$, 20), 245 ($SFe_2C{\equiv}CPh$, 36), 276 ($HSFe_3Ph$, 20), 224 ($SFe_3C{\equiv}C$, 6), 200 (SFe_3, 13), 189 ($SFeC{\equiv}CPh$, 14), 144 (SFe_2, 17), 102 ($PhC{\equiv}CH$, 15), 57 (^{t}Bu, 28), 56 (Fe, 19).

Reaction of (μ-σ,π-C≡C^{t}Bu)(μ-^{t}BuS)$Fe_2(CO)_6$ with $Fe_2(CO)_9$. In an experiment similar to the reaction of 3 with diiron nonacarbonyl, a toluene solution containing 0.98 g (2.17 mmol) of (μ-σ,π-C≡C^{t}Bu)(μ-^{t}BuS)$Fe_2(CO)_6$ (**5**) and 1.57 g (4.31 mmol) of diiron nonacarbonyl was stirred for 34 h at room temperature. Removal of the solvent in vacuo left a dark oil which was purified by column chromatography under nitrogen. Hexane eluted brownish red and dark green bands which were contiguous. The best separation possible was made. The brownish red band was not collected while the dark green band gave 1.22 g of a greenish, oily solid. (After this greenish, oily solid had been dried in vacuo for several hours, it had changed color to red.) Recrystallization from pentane yielded 0.65 g (1.10 mmol, 51%) of (μ_3,η^2-C≡C^{t}Bu)(μ-^{t}BuS)$Fe_3(CO)_9$ (**9**) as an air-stable, *red* solid, mp 91.0–98.0 °C. When in solution, this red compound converts partially to a green product, possibly of type 11, identified by TLC. However, when the solvent is removed in vacuo, a red compound again remains. Although the solid state structure is that shown in eq 5, in solution both structures of type 9 and 11 may be in equilibrium. Consequently, the IR and NMR spectra reflect the presence of both of these isomers in solution.

Anal. Calcd for $C_{19}H_{18}Fe_3O_9S$: C, 38.68; H, 3.08. Found: C, 38.72; H, 3.03. IR (CCl_4): 1710 w (C≡C); terminal carbonyl region (pentane) 2080 m, 2045 vs, 2025 vs, 2010 vs, 1988 s, 1982 sh, 1970 m cm^{-1}. ^1H NMR (CD_2Cl_2, 300 MHz): δ 1.16 (s, 9 H, $C(CH_3)_3$ first isomer), 1.52 (s, 9 H, $C(CH_3)_3$ second isomer), 1.75 (s, 18 H, $C(CH_3)_3$ both isomers). ^{13}C NMR (CD_2Cl_2, 67.9 MHz): δ 30.83 (q, J = 127.0 Hz, $C(CH_3)_3$), 31.23 (q, J = 127.2 Hz, $C(CH_3)_3$), 33.10 (q, = 127.3 Hz, $C(CH_3)_3$—roughly twice the intensity of the other *tert*-butyl resonances), 44.16 (s, $C(CH_3)_3$), 45.95 (s, $C(CH_3)_3$), 49.38 (s, $C(CH_3)_3$), 149.49 (s, acetylide C), 202.40 (s, acetylide C), 211.50, 211.93, and 212.69 (all s, Fe–CO), 215.14 (s, acetylide C), 220.21 (s, acetylide C). Mass spectrum (EI): m/z (relative intensity) 590 (M^+, 1), 562 (M^+ – CO, 4), 534 (M^+ – 2CO, 12), 506 (M^+ – 3CO, 8), 478 (M^+ – 4CO, 7), 450 (M^+ – 5CO, 24), 422 (M^+ – 6CO, 16), 394 (M^+ – 7CO, 26), 366 (M^+ – 8CO, 38), 338 (M^+ – 9CO, 18), 282 ($HSFe_3C{\equiv}C^tBu$, 52), 226 ($HSFe_3C{\equiv}CH$, 52), 200 (SFe_3, 25), 169 ($HSFe_2C{\equiv}C$, 17), 144 (SFe_2, 15), 57 (^{t}Bu, 50), 56 (Fe, 26).

Acknowledgment. We are grateful to the National Science Foundation for generous support of the preparative work carried out at MIT and to the Natural Sciences

and Engineering Research Council of Canada (NSERC) and the University of Alberta for the structural study at the University of Alberta. In addition M.C. thanks NSERC for partial funding of the diffractometer and A.D.H. thanks NSERC and the Izaak Walton Killam Foundation for postdoctoral fellowships. We thank also the MIT Mass Spectrometry Facility (supported by NIH Division of Research Resources, Grant No. RR00317; K. Biemann, principal investigator) for mass spectra.

Registry No. 1, 115796-06-0; 2, 115796-07-1; 3, 115796-08-2; 4, 115796-11-7; 5, 115796-09-3; 6, 115796-10-6; 7, 115796-12-8; 8, 115796-13-9; 9, 115796-14-0; dicobaltoctacarbonyl, 10210-68-1; diiron nonacarbonyl, 15321-51-4; iron, 7439-89-6; cobalt, 7440-48-4.

Supplementary Material Available: Tables of anisotropic thermal parameters, idealized hydrogen parameters, and weighted least-squares planes (19 pages); listings of observed and calculated structure amplitudes (74 pages). Ordering information is given on any current masthead page.

Fluxional Behavior of Iron Complexes of 1,2-Cycloheptadiene: The Role of the Allyl Cation

Su Min Oon and W. M. Jones*

Department of Chemistry, University of Florida, Gainesville, Florida 32611

Received February 8, 1988

The fluxional behavior of two iron complexes of 1,2-cycloheptadiene—$(\eta^5\text{-}C_5H_5)(CO)_2Fe(\eta^2\text{-}1,2\text{-}$cycloheptadiene)fluoroborate (**5**) and its Ph_3P-substituted relative **13**—has been studied. At this time, we report evidence for (1) fluxionality of **5** by a Vrieze–Rosenblum mechanism (E_a = 13.9 kcal/mol), a mechanism where the chirality of the allene moiety is retained, (2) fluxionality of **13** by the same mechanism with an activation barrier about 3–4 kcal/mol higher than that for **5**, (3) accessibility of an allyl cation mechanism in the latter case with E_a = ca. 23 kcal/mol, and (4) circumstantial evidence for accessibility of an allyl cation (E_a between 14.2 and 22 kcal/mol) from **5**.

The fluxionality of transition-metal complexes of allenes in which the metal migrates between the double bonds has piqued the curiosity of chemists since Ben-Shoshun and Pettit[1] first observed this behavior in the tetracarbonyliron complex of tetramethylallene. Although, to date, there are not enough examples to make sweeping generalities, examples of Pt(0),[2] Ni(0),[3] and Pt(II)[4] complexes have been reported that do not show this behavior on the NMR time scale at moderate temperatures (typically near room temperature), Pd(0)[5] complexes have been found that show fluxionality on this time scale but by a dissociation–recombination mechanism, and Fe(II)[6] cationic and Pt(II)[7] neutral complexes have been found that undergo intramolecular fluxionality at rates that are rapid enough to be detected by ^1H NMR.

Two mechanisms have been considered for the intramolecular fluxional process. Their transition states are pictured in **1**[6,7b] and **2**.[8] To distinguish between these is relatively straightforward, because **1** retains the chirality

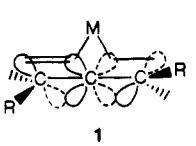

1

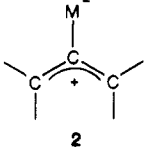

2

Scheme I

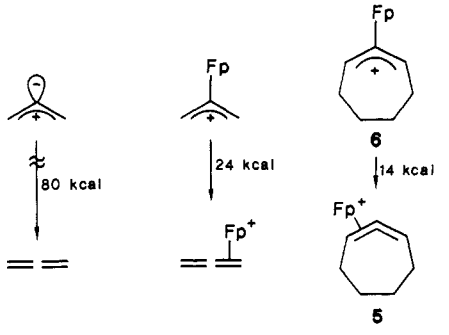

of the allene ligand during the fluxionality process while it would ultimately be lost if it went via transition state **2**.[9] Thus, Rosenblum's[6] finding that the Fp^+ [Fp = dicarbonyl(η^5-cyclopentadienyl)iron] complex of optically active 1,2-cyclononadiene did not racemize under conditions where fluxionality was rapid is inconsistent with the second mechanism for the fluxional behavior of Fp^+ complexes of allenes. The second transition state **2** has been invoked only once, when Cope[8] suggested it as a way to explain the mutarotation of **3** (Am = active amine). However, Rosenblum[6] has challenged this mechanism by pointing out that the racemization could be equally well

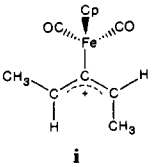

i

(1) Ben-Shoshan, R.; Pettit, *R. J. Am. Chem. Soc.* **1967**, *89*, 2231.
(2) (a) Otsuka, S.; Nakamura, A.; Tani, K. J. *Organomet. Chem.* **1968**, *14*, 30. (b) Winchester, W. R.; Jones, W. M. *Organometallics* **1985**, *4*, 2228.
(3) Otsuka, S.; Tani, K.; Yamagata, T. *J. Chem. Soc., Dalton Trans.* **1973**, 2491.
(4) (a) Briggs, J. R.; Crocker, C.; McDonald, W. S.; Shaw, B. L. *J. Chem. Soc., Dalton Trans.* **1981**, 121. (b) Clark, H. C.; Manzer, L. E. *J. Am. Chem. Soc.* **1985**, *95*, 3812.
(5) Otsuka, S.; Nakamura, A. *Adv. Organomet Chem.* **1976**, *14*, 245.
(6) Foxman, B.; Marten, D.; Rosan, A.; Raghu, S.; Rosenblum, M. *J. Am. Chem. Soc.* **1977**, *99*, 2160.
(7) (a) Vrieze, K.; Volger, H. C.; Gronert, M.; Pratt, A. P. *J. Organomet. Chem.* **1969**, *10*, 19. (b) Vrieze, K.; Volger, H. C.; Pratt, A. P. *J. Organomet. Chem.* **1970**, *21*, 467.
(8) Cope, A. C.; Moore, W. R.; Bach, R. D.; Winkler, H. S. *J. Am. Chem. Soc.* **1970**, *92*, 1243.
(9) Chirality is not necessarily lost when **2** is formed. For instance, *i* is chiral, and if it were to collapse before rotation around the carbon iron bond, the resulting allene complex would not necessarily be racemic. However, multiple passes through **i** should lead to racemization.

0276-7333/88/2307-2172$01.50/0